

Mechanical Performance Enhancement of Alkali-Activated Composites Using Synthetic Fibers with Metazeolite and Aluminum Sludge-Based Recycled Concrete Aggregates

Beyza Fahriye Aygün^{*}, Mücteba Uysal^{**}, Ramazan Çingi^{*}

^{*} Department of Civil Engineering, Istanbul University-Cerrahpasa, Üniversite Yolu No:2, 34320 Avcılar, Istanbul, Türkiye.

^{**} Department of Civil Engineering, Yıldız Technical University, Davutpasa 34360, Esenler, Istanbul, Türkiye.

(beyza.aygun@ogr.iuc.edu.tr ; mucteba@yildiz.edu.tr ; ramazancingi@hotmail.com)

Received: 18.05.2024 Accepted: 06.11.2024

Abstract- This study examines the substantial enhancement in the performance of alkali-activated composites (AACs) produced from a distinctive combination of metazeolite (MZ) and slag (S), reinforced with synthetic fibers, and augmented with aluminum sludge (AS) and recycled concrete aggregate (RCA). The composites were subjected to activation through the use of a specific sodium hydroxide (NaOH) and sodium silicate (Na_2SiO_3) blend in a 2:1 ratio, with an activator-to-binder ratio of 0.95. Through a process of experimentation, the research team identified an optimal mix by varying the molarities of sodium hydroxide (NaOH) between 8M and 14M and the ratios of metazeolite to slag between 25% and 100%. The aforementioned mixture, comprising 50% MZ and 50% S, was activated with 12M NaOH and enhanced with 30% aluminum sludge, exhibiting remarkable strength characteristics. Furthermore, the incorporation of synthetic fibres, including polyethylene (PEF), polyamide (PAF), and basalt fibers (BF), resulted in a notable enhancement of the material's performance. It is noteworthy that the addition of basalt fibers at a concentration of 0.5% resulted in a 7% increase in compressive strength and a 24% improvement in flexural strength. This pioneering research illuminates the transformative potential of MZ-S-based AACs, particularly when combined with AS and BF, paving the way for the development of sustainable construction materials that meet contemporary performance and environmental standards.

Keywords: Alkali-activated composites, Metazeolite, Synthetic fibers, Mechanical properties

1. Introduction

In recent years, there has been a notable increase in the advocacy for sustainable development in civil engineering, driven by the growing necessity for eco-friendly and cost-efficient construction materials. The prevailing construction methodologies rely predominantly on Portland cement (PC), which has a considerable environmental impact, accounting for approximately 7% of global CO_2 emissions. In light of the industry's pursuit of more sustainable alternatives, alkali-activated composites (AACs) have emerged as a promising solution, offering a reduction in CO_2 emissions and lower energy consumption. This study examines the innovative

application of metazeolite (MZ) and slag (S) in AACs, which are further enhanced with aluminum sludge (AS) and recycled concrete aggregate (RCA) to create high-performance, sustainable building materials. The phenomenon of urbanization has resulted in a notable increase in construction and demolition activities, which in turn has led to a considerable rise in waste generation. In regions prone to seismic activity such as Turkey, urban transformation projects are anticipated to result in the generation of approximately 2 billion tons of construction waste over the next two decades. This scenario presents a unique opportunity to recycle such waste into valuable construction materials, thereby addressing both

environmental and economic concerns. The utilisation of recycled aggregates in AACs serves to alleviate waste disposal issues whilst simultaneously reducing the demand for virgin raw materials, thereby aligning with the overarching objectives of sustainable development. Incorporation of diverse fibers has been demonstrated to markedly enhance the mechanical properties of AACs. The integration of synthetic fibers, such as polyethylene (PEF), polyamide (PAF), and basalt fibers (BF), has shown significant promise. These fibers strengthen the structural integrity of AACs by enhancing tensile and flexural strengths, minimizing crack propagation, and improving overall durability. Sahin et al. [3] examined the effects of different basalt fiber ratios in MK-based AACs with various aggregate types. While the mechanical strengths remained within acceptable limits, AACs containing recycled aggregate exhibited slightly reduced properties. In a study by Sahin et al. [3], the effects of varying basalt fiber ratios in MK-based AACs with different aggregate types were examined. While the mechanical strengths remained within acceptable limits, AACs containing recycled aggregate exhibited slightly reduced properties. The unique chemical structures of natural zeolites render them indispensable in the geopolymerization process of AACs. The calcination of these materials at specific temperatures enhances their reactivity, thereby facilitating the formation of robust and durable composites. Zheng et al. [4] conducted a comparative analysis of the frost resistance of concrete using calcined zeolite, demonstrating that the porosity and pore structure exhibited improved characteristics with increasing curing age. Similarly, Florez et al. [5] investigated the calcination-pre-grinding processes of zeolite, revealing enhanced pozzolanic properties. Nikolov et al. [6] employed calcined natural zeolite and clinoptilolite as AAC precursors, resulting in the attainment of considerable compressive strength through potassium silicate activation. Further studies by Ozen and Alam [7] emphasized the significance of activator ratios in the geopolymerization of zeolite-based AACs. Aygörmöz [8] conducted an analysis of the high-temperature effects of MK-S-based AACs reinforced with basalt fiber, demonstrating that these materials remain stable even after exposure to temperatures as high as 750 °C. Integrating aluminum sludge (AS) into AACs offers a novel approach to waste management and material enhancement. AS, a by-product of alumina production, is generally seen as a disposal challenge due to its fine particle size and potential environmental impact. However, its inclusion in AACs can aid in setting and enhancing compressive strength, making it a valuable component in sustainable construction materials. This study provides a comprehensive analysis of the synergistic effects of AS and fiber reinforcement in AACs, focusing on their mechanical properties and durability. The combination of zeolite and fibers results in enhanced compressive strength and abrasion resistance. Investigations into ultra-high-performance AACs (UHPAACs) with PPF and SF have shown improved mechanical properties, especially with PPF in SF samples. Non-destructive testing methods, such as UPV, have been used to evaluate SF-reinforced concrete containing recycled nylon granules and zeolite, demonstrating enhanced properties [9-29]. The use of

steel fibers (SF) and basalt fibers (BF) has proven effective in boosting the workability and strength of alkali-activated materials (AAMs) or AACs. The concurrent utilization of SF and BF results in a synergistic enhancement in the hardening process, a reduction in stress concentration, and the limitation of crack formation. While SFs enhance the internal structure and properties of the material, BFs facilitate the formation of a well-defined interfacial region, thereby improving water absorption and porosity. By embedding these fibers into adaptable composite materials, it is possible to achieve peak performance while keeping costs low, thus advancing environmental sustainability. Furthermore, the incorporation of natural fiber reinforcement into traditional composites represents a viable and sustainable approach that is environmentally and economically advantageous. The potential of different fibers to enhance the properties of AAC has been investigated by various researchers. In their study, Choi et al. [30] demonstrated that the incorporation of PEF-PVAF reinforcement in S-based AACs resulted in enhanced tensile capacity and healing performance compared to PEF alone. In a related study, Wang et al. investigated the effects of PVAF and nano-silica on MK-S-based AACs, observing significant improvements in strength and durability with optimal PVAF and NS mixtures. In a study by Shaikh [31], PPF was investigated as a reinforcement fiber. The findings indicated that PPF composites exhibited superior mechanical properties with an optimal fiber content of 0-1% by volume.

This study elucidates the eco-technological advantages of sustainable AACs in the construction industry. The global construction industry is a significant contributor to environmental pollution and greenhouse gas emissions, primarily due to the extensive usage of PCs and the accumulation of solid waste. Developed countries have implemented regulatory measures with the objective of controlling PC emissions and promoting the recycling of waste concrete. The importance of recycling cannot be overstated, particularly in light of the significant environmental impact of debris resulting from earthquakes and urban transformations. This research underscores the significance of sustainable AAC production, illustrating the ecological advantages.

2. Materials and Methods

In this study, various materials were employed to create the alkali-activated composites (AACs). Slag (S), obtained from the Bolu Cement Industry, was used due to its high specific gravity (SG) of 2.9 and an impressive 98.6% pass rate through a 45-micron sieve. Mec Energy supplied the zeolite, characterized by a specific gravity of 2.17 and a significant surface area of 9660 cm²/g. The zeolite underwent calcination at 900 °C to enhance its reactivity. Aluminum sludge (AS) was procured from Eti Aluminum AS, dried at 105 °C, and milled to a 90 µm particle size. Recycled concrete aggregate (RCA), provided by a local recycling company, featured an SG of 2.05 and was sieved through a 2 mm sieve to obtain fine aggregates. The chemical activators used included NaOH with a purity exceeding 99% and Na₂SiO₃ containing 27.2% SiO₂, 8.2% Na₂O, with a pH range

of 11-12.4. Table 1 presents the chemical compositions of these binder materials. AACs were formulated with a sand-to-binder ratio of 2.5 and an activator-to-binder ratio of 0.95. The weight ratio of Na_2SiO_3 to NaOH was maintained at 2:1, in line with both literature guidelines and preliminary laboratory tests. The initial phase involved creating 16 different AAC mixes, categorized into four series based on varying binder compositions: 100% MZ, 75% MZ + 25% S, 50% MZ + 50% S, and 75% S + 25% MZ. Each series was tested with four NaOH molarities: 8M, 10M, 12M, and 14M.

The mix that demonstrated the highest strength in this phase underwent further testing with the addition of 10%, 20%, and 30% AS to assess its impact on compressive strength, flexural strength (at 7 and 28 days) and water absorption ratios (at 28 days). In (0.5%, 1%, 1.5%, and 2%) was analyzed for their mechanical properties (Table 2). The final phase, based on the optimal mix of MZ-S and AS, the influence of synthetic fibers—basalt fibers (BF), polyethylene fibers (PEF), and polyamide fibers (PAF)—at various percentages.

Table 1. Chemical composition binder materials.

Component	Slag (%)	Metazeolite (MZ) (%)	Red Mud (RM) (%)	RCA (%)
SiO ₂	40.55	76.90	16.20	62.56
Al ₂ O ₃	12.83	13.50	22.90	12.52
Fe ₂ O ₃	1.10	1.40	34.50	5.82
TiO ₂	0.75	0.10	-	0.75
CaO	35.58	2.00	1.80	12.0
MgO	5.87	1.10	-	1.83
K ₂ O	0.68	3.50	-	1.30
Na ₂ O	0.79	0.30	8.70	2.69
LOI	0.03	1.10	-	-
MnO	-	0.10	-	0.12

Table 2. Mixture contents and quantities.

	MZ (g)	AS (g)	S (g)	RCA (g)	Na ₂ SiO ₃ (g)	NaOH (g)	PEF (g)	PAF (g)	BF (g)
100MZ	450	-	-	1125	142.5	285	-	-	-
75MZ+25S	337.5	-	112.5	1125	142.5	285	-	-	-
50MZ+50S (C)	225	-	225	1125	142.5	285	-	-	-
75S+25MZ	112.5	-	337.5	1125	142.5	285	-	-	-
50MZ+50S+10AS	225	112.5	225	1012.5	142.5	285	-	-	-
50MZ+50S+20AS	225	225	225	900	142.5	285	-	-	-
50MZ+50S+30AS	225	337.5	225	787.5	142.5	285	-	-	-
C+30AS+0.5PEF	225	337.5	225	783.2	142.5	285	4.28	-	-
C+30AS+1PEF	225	337.5	225	774.7	142.5	285	8.55	-	-
C+30AS+1.5PEF	225	337.5	225	761.85	142.5	285	12.82	-	-
C+30AS+2PEF	225	337.5	225	744.75	142.5	285	17.1	-	-
C+30AS+0.5PAF	225	337.5	225	784.09	142.5	285	-	3.41	-
C+30AS+1PAF	225	337.5	225	781.22	142.5	285	-	6.82	-
C+30AS+1.5PAF	225	337.5	225	764.44	142.5	285	-	10.23	-
C+30AS+2PAF	225	337.5	225	748.20	142.5	285	-	13.65	-
C+30AS+0.5BF	225	337.5	225	734.63	142.5	285	-	-	10.12
C+30AS+1BF	225	337.5	225	763.84	142.5	285	-	-	20.25
C+30AS+1.5BF	225	337.5	225	750.85	142.5	285	-	-	30.37
C+30AS+2BF	225	337.5	225	723.94	142.5	285	-	-	40.5

To evaluate the mechanical properties of the AACs, both cubic (50x50x50 mm) and prismatic (40x40x160 mm) samples were prepared. Compressive and flexural strengths were measured using an automatic testing machine following the relevant standards. For water absorption tests, as per ASTM C 642, the oven-dried samples were weighed and then immersed

in water for 48 hours to achieve saturation before being reweighed. Flexural strength was assessed on the 28th day using a single-point loading method in a standardized testing setup (Fig. 1.).



Fig. 1. Images of the experimental setup and specimen testing process, including preparation, testing, and storage of AACs.

3. Results and Discussion

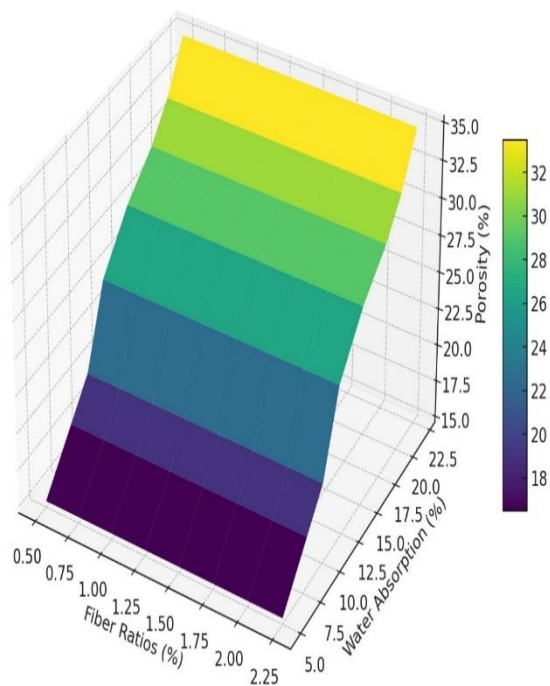


Fig. 2. Water absorption and void ratio values of fiber-reinforced AACs at 28 days.

The detailed analysis of the relationships among fiber ratios, water absorption, and porosity in construction materials provides crucial insights into the behavior of AAC compositions under various fiber concentrations and the inclusion of AS. The observed linear progressions in the fiber ratios versus water absorption and porosity Fig. 2. underline a significant influence of incremental increases in fiber content on these essential material properties, reflecting both opportunities and challenges in material design for construction applications. Starting with the relationship between fiber ratios and water absorption, the upward trajectory from 0.5% to 2.25% fiber content, leading to an increase in water absorption from about 5% to over 22%, highlights a critical point: while increased fiber content enhances certain material properties, it also raises water absorption significantly. This observation is particularly relevant in environments prone to moisture or direct water exposure, where high water absorption could undermine material integrity. However, the graph also suggests a saturation point at around 2.0% fiber ratio, beyond which water absorption does not decrease, indicating a threshold where additional fibers may contribute to increased porosity rather than enhancing water resistance. Regarding porosity, the similarly ascending trend as fiber content increases suggests that higher fiber concentrations may offer benefits such as improved insulation properties or reduced material density but also introduce greater porosity. This increased porosity could weaken the material's structural strength, making it less suitable for load-bearing applications unless compensatory design measures are implemented. However, the optimal fiber ratio, evidenced around 1.0%, effectively balances the dual needs of reduced water absorption and

lower porosity, achieving a denser and more robust matrix. Further analysis incorporating 10% and 20% AS in the AAC matrix indicates that these additions significantly reduce water absorption through chemical interactions, likely involving the CaO/CaSO₄ composite activator, which promotes the formation of long-chain Si-O-Al-O structures that density the matrix and reduce porosity. Yet, at 30% AS, the benefits diminish as water absorption increases, suggesting a detrimental oversaturation effect that could introduce microstructural weaknesses. BFs merge as particularly effective among various fiber types analyzed, demonstrating the lowest water absorption and porosity across all ratios, indicating their superior reinforcement capabilities within the AAC matrix. PEFs at 1% significantly enhance matrix densification, aligning with findings from Sahin et al. [3], which noted a rapid decrease in porosity at a 0.4% PEF ratio but found diminishing returns at higher concentrations.

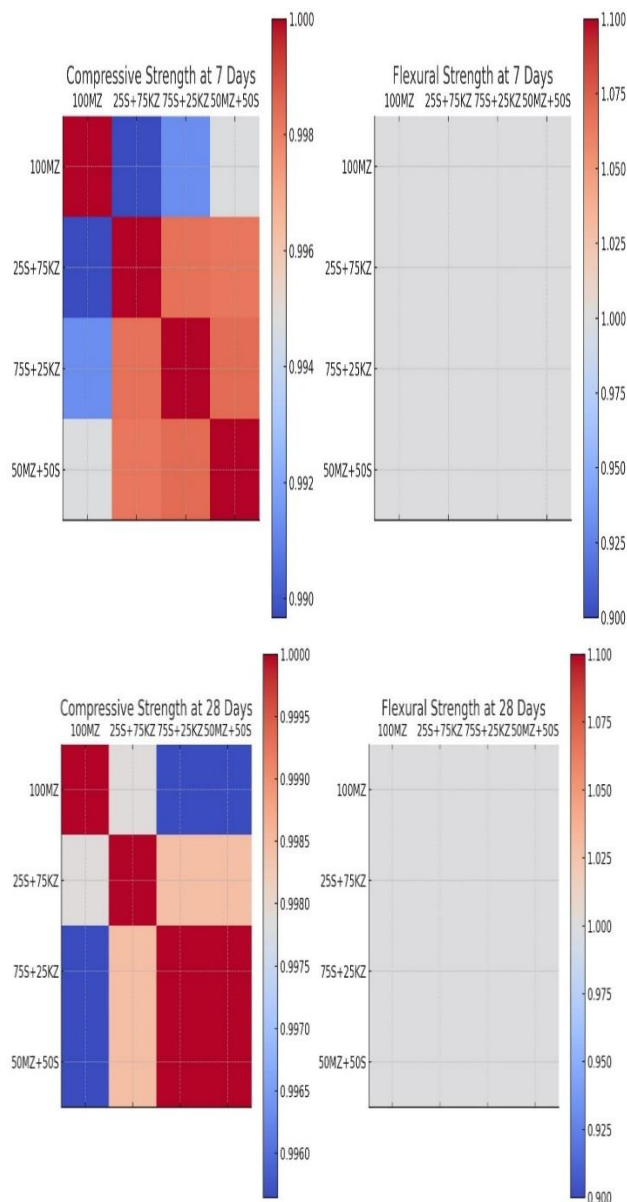


Fig. 3. Compressive and flexural strengths of AACs of different molarity and mixing ratios at 7 and 28 days.

Prior to the commencement of further testing, trial mixtures were prepared with varying compositions and molar ratios. The series exhibiting the highest compressive and flexural strengths was selected for detailed physical and mechanical property evaluations. Subsequent experiments were conducted to investigate the effects of adding 10%, 20%, and 30% AS to the optimized series. Fig. 3. illustrate the anticipated positive correlation between NaOH concentration and compressive and flexural strengths, with peaks observed at 12M before a slight decline at 14M. When subjected to different molarity levels, each of these mixtures demonstrated almost perfect correlation coefficients, indicating highly predictable strength properties under controlled alkaline conditions. At 7 days, the correlation coefficients for compressive strength ranged from 0.989 to 1.000, highlighting an almost uniform rate of chemical reaction and strength development across these varied compositions. This suggests that the initial curing phase rapidly stabilizes material properties, which is crucial for early-stage structural applications. The flexural strength at this early stage also showed perfect correlations (1.0), indicating a uniform resistance to bending forces across all tested mixtures, a critical factor for ensuring the material's reliability in structural components under flexural stress. By 28 days, the materials continued to exhibit strong correlations in compressive strength, with coefficients from 0.995 to 1.000, confirming that the compositions reached a state of chemical equilibrium or full reaction maturity, reflecting the standard industry practice of using a 28-day curing period to assess material strength for structural applications. The perfect correlation in flexural strength across mixtures at 28 days reinforces the materials' consistent performance. It underscores their suitability for diverse construction needs where long-term durability and resistance to mechanical stress are required. This analysis underscores the predictability and reliability of these material mixtures in achieving specified strength characteristics, which are essential for optimizing construction processes and enhancing structural safety. The ability to anticipate how different compositions respond to changes in molarity allows engineers to tailor materials to specific environmental conditions and structural requirements, streamlining construction timelines and potentially reducing costs. Furthermore, this insight into material behavior supports ongoing efforts to refine construction materials for improved performance, ensuring that structures meet and exceed safety and durability standards. Similar trends have been observed by Malkawi et al. [32] and Chaithanya et al. [33] in AACs containing fly ash (FA) or S. These findings are consistent with those of Singh et al. [34] and Mudgal et al. [35], who also identified optimal AS levels for improved strength and compactness in AACs. The presence of AS is conducive to geopolymerization, which likely contributes to a higher Si/Al and Na/Al molar ratio, thereby enhancing densification and strength. Aygörmez [36, 37] reported similar improvements in AAC mortars, achieving a 12% increase in compressive strength with 25% AS replacement. Notably, Zakira et al. [38] achieved even higher strengths (66 MPa) using 50% AS, which highlights the potential of AS for high-performance AACs. The incorporation of AS appears to optimise the

internal microstructure of the AACs, promoting a more homogeneous and dense matrix. This densification is of great importance for improving the mechanical properties of the material, as it reduces the number of internal voids and enhances the overall bonding within the material. The findings indicate that AS additions up to 20% result in significant improvements in mechanical performance, in alignment with the studies by Singh et al. [34] and Mudgal et al. [35], which reported similar enhancements in AAC properties with optimal AS levels. Beyond this threshold, at 30% AS, the benefits appear to diminish, likely due to the oversaturation effect, which may lead to increased porosity or the formation of less desirable phases within the matrix. This observation highlights the significance of optimizing the content of supplementary materials, such as AS, to achieve a balance between maximizing strength and maintaining structural integrity. This is consistent with the research by Aygörmez [36, 37], which noted significant long-term strength improvements with AS incorporation. The superior performance of the 75S+25MZ mixture at 12M NaOH can be attributed to several factors, including the optimal dissolution of aluminosilicates, the balanced Na/Al and Si/Al ratios, and the effective densification of the matrix. The presence of slag contributes to long-term strength due to its latent hydraulic properties, which continue to enhance the matrix even after the initial curing period. This is consistent with the findings of Chaithanya et al. [33], who also observed long-term strength gains in AACs with slag. The incorporation of fibers at specific ratios serves to enhance the mechanical properties of the material, as it improves the internal bonding and reduces microcracking. The findings indicate that a 1.0% fiber ratio is optimal for both compressive and flexural strengths, as it provides the most optimal balance between fiber reinforcement and matrix integrity. The positive correlation between NaOH concentration and mechanical properties up to 12M is well-supported by the literature, with similar trends observed in studies by Malkawi et al. [32] and Singh et al. [34]. The observed trend of increasing strength with higher molarity up to 12M is consistent with the findings of Malkawi et al. [32], who reported that higher NaOH concentrations improve the dissolution of aluminosilicate precursors, leading to a denser and stronger matrix. Nevertheless, the slight decline in strength at 14M may be attributed to the excessive alkali content, which may result in the formation of alkali carbonates or other secondary phases that do not contribute to strength development. At 28 days, the compressive strength trends remain consistent with the 7-day results. The 75S+25MZ mixture continues to demonstrate superior performance, achieving compressive strengths exceeding 50 MPa at 12M NaOH. This sustained strength gain over time indicates a stable and ongoing geopolymerization process. The presence of slag in the mixture enhances the long-term strength due to its latent hydraulic properties, which contribute to continued strength development beyond the initial curing period. Similarly, Chaithanya et al. [33] observed comparable long-term strength gains in AACs with S, underscoring the significance of slag content in attaining high-performance composites. Flexural strength is a crucial parameter that reflects the material's capacity to withstand bending and cracking. The

flexural strength at seven days follows a similar trend to compressive strength, with the 75S+25MZ mixture exhibiting the highest values. This finding is consistent with the findings of Singh et al. [34], who reported that optimal AS levels and fiber reinforcement significantly enhance the flexural strength of AACs. The 28-day flexural strength results serve to reinforce the superiority of the 75S+25MZ mixture. At 12M NaOH, the flexural strength exceeds 20 MPa, indicating excellent durability and resistance to bending stresses over time. The slight decline observed at 14M molarity is consistent with the compressive strength results, suggesting that excessively high NaOH concentrations may have an adverse effect on the matrix structure. Mudgal et al. [35] also observed that while higher alkali concentrations enhance early strength, they can lead to long-term durability issues if not optimized.

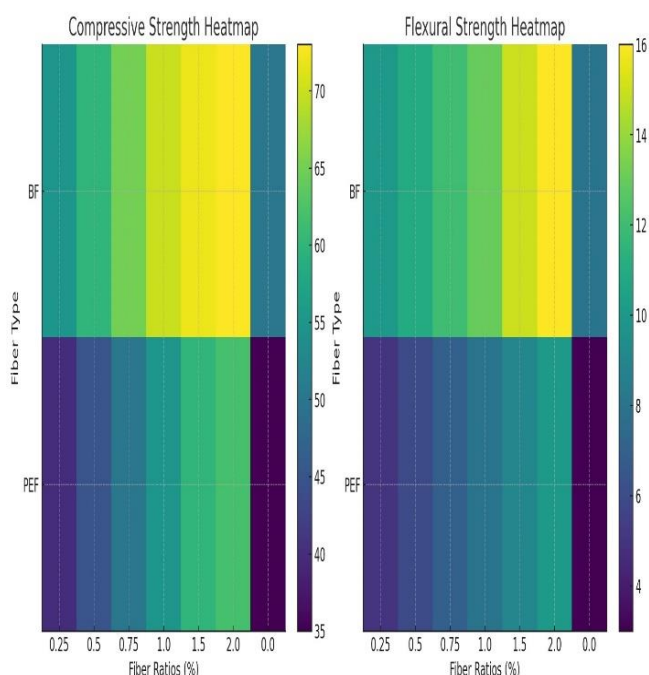


Fig. 4. Compressive and flexural strengths of AACs in different synthetic fibers and ratios at 28 days.

The data presented in Fig. 4 indicates that PEFs were beneficial only up to a 1% addition, achieving a maximum compressive strength of 47.06 MPa before experiencing a significant decline. This decline can be attributed to the phenomenon of fiber agglomeration at higher concentrations, which leads to poor dispersion and the creation of weak points within the matrix. The heatmaps vividly illustrate the compressive and flexural strengths of construction materials integrated with BF and PEFs, providing a clear visual distinction across various fiber ratios from 0.25% to 2.00%, including a control sample without fibers. This analysis serves not only as a comparative overview but also as a deep dive into the material science implications of fiber reinforcement in cementitious composites. Starting with the compressive strength, the heatmap gradients—transitioning from deep purples to vibrant yellows—indicate increasing strength levels as the fiber content rises. Particularly, BFs exhibit

superior performance over Polyethylene Fibers, underscored by consistently higher values across all fiber ratios. This distinction could be attributed to the inherent mechanical properties of basalt fibers, which include high tensile strength and stiffness. These properties effectively transfer stress across the fiber-matrix interface, enhancing the composite's overall load-bearing capacity. The presence of basalt fibers potentially initiates a more efficient crack distribution mechanism, which helps in arresting cracks at early stages, thereby improving the compressive strength. On the other hand, PEFs, while still enhancing strength, offer a different set of benefits and challenges. These synthetic fibers are known for their flexibility and high strain capacity, which contribute positively to the energy absorption capabilities and toughness of the concrete. However, their lower modulus compared to basalt fibers might explain the lesser improvement in compressive strength, as they do not contribute as effectively to the stiffness of the composite. Nevertheless, their inclusion in the composite matrix still offers valuable enhancements, particularly in applications where flexibility and impact resistance are desirable. The flexural strength heatmap further explores the dynamic between fiber content and bending resistance. Again, the visual gradient reflects an increase in strength with higher fiber ratios, with BFs leading in performance enhancement. In flexural applications, the role of fibers is critical as they bridge cracks that might otherwise propagate under bending stress, thereby maintaining the integrity of the material under load. The effective distribution and bonding of basalt fibers within the matrix can significantly increase the material's resistance to bending, highlighting their suitability for structural applications where flexural stresses are prevalent. The control samples, noticeably lower in strength in both heatmaps, underscore the significant role that fibers play in enhancing concrete properties. The contrast between the fiber-enhanced samples and the control illustrates the effectiveness of fiber integration, providing a stark visualization of the material advancements achievable through fiber technology. Similarly, Uysal et al. [39] observed enhancements in mechanical properties with various fibers in AS-MK-AACs. The researchers observed that PVAFs effectively increased flexural strength by 61% compared to the control, indicating the potential of synthetic fibers in enhancing AACs' mechanical performance. The enhanced performance of BFs can be attributed to their intrinsic properties and the synergistic interactions with the AAC matrix. BFs, derived from volcanic rock, exhibit excellent mechanical properties, including high tensile strength, chemical resistance, and thermal stability. These properties render BFs particularly suitable for reinforcing AACs, as they can withstand the alkaline environment and high temperatures associated with geopolymerization. The compatibility of BFs with the AAC matrix ensures effective stress transfer and crack bridging, which results in significant improvements in compressive strength. The fiber bridging effect, whereby fibers span across cracks and transfer stress, plays a pivotal role in regulating crack formation and development. As the fibers bridge the cracks, they effectively arrest crack growth

and enhance the load-bearing capacity of the AACs. The flexural strength of the composites increased modestly with fiber reinforcement, with an improvement of approximately 0.5% observed for both PEF and PAF at a fiber content of 0.5%. However, the incorporation of BF at the same 0.5% ratio yielded a substantial improvement of 12.61%, which highlights the superior reinforcing capabilities of BFs. It is noteworthy that when the PEF content was increased to 1%, the flexural strength exhibited a higher value of 10.54 MPa. Notwithstanding this increase, the strength remained below the control value of 12.34 MPa. This trend indicates that while PEFs can enhance flexural strength at certain ratios, they may not be as effective as other types of fibers, such as BF, especially at higher concentrations. The observed pattern of initial strength increase followed by a decline at higher fiber contents is consistent with findings from other studies, including those by Alomayri et al. [40, 41], who investigated cotton fiber-reinforced FA-based AACs (FA-AACs). A similar trend was observed, whereby the flexural strength initially increased with fiber content up to 0.5%, but declined beyond this point. This behavior can be attributed to optimal fiber dispersion at lower ratios, which facilitates effective stress transfer. In contrast, higher fiber contents can lead to agglomeration and inhomogeneous distribution within the matrix. The superior performance of BF at 0.5% can be attributed to its intrinsic mechanical properties and its interaction with the geopolymer matrix. Basalt fibers are renowned for their high tensile strength, excellent chemical resistance, and thermal stability, rendering them optimal for reinforcing AACs. The robust bond between BFs and the AAC matrix ensures efficient stress transfer and crack bridging, significantly enhancing the material's flexural strength. This is corroborated by the findings of Baykara et al. [42], who observed that PPF-reinforced AACs also exhibited optimal performance at 0.5% fiber content. Beyond this optimal ratio, the performance declined due to potential issues such as fiber inhomogeneity and agglomeration, which compromise the matrix integrity and lead to the formation of weak points.

4. Conclusions

In the exploration of optimized AACs, the study reveals significant enhancements in mechanical properties through various additives and modifications. AAC mixture comprising 50% MZ and 50% S, augmented with 30% AS at a 12M NaOH concentration, exhibited an exceptional compressive strength of 61.85 MPa, demonstrating the efficacy of high molarity and specialized components in achieving superior strength. Furthermore, the addition of BFs at just a 0.5% ratio not only increased the compressive strength by 7.26% but also significantly boosted the flexural strength by 24.15%, highlighting BF's remarkable reinforcing capabilities. Conversely, PEFs, used at a 1% ratio, enhanced the flexural strength to 10.54 MPa, yet this figure still fell below the control mix's strength, indicating a nuanced interplay between fiber type and concentration in AAC performance. Additionally, the mixture of 75% Slag with 25% Metazeolite consistently showed the highest compressive strength across all tested molarity levels,

particularly achieving around 50 MPa at a 12M NaOH concentration within 7 days. This composition maintained its peak strength over 28 days, underscoring its robustness. However, an increase in Aluminum Sludge content to 30% resulted in higher water absorption, suggesting a threshold beyond which additional AS is counterproductive. This intricate study not only underscores the importance of precise component ratios and types in AAC but also provides a roadmap for tailoring AAC properties to meet specific structural requirements effectively.

References

- [1] M. Lakew, O. Canpolat, M. M. Al-Mashhadani, M. Uysal, A. Niş, Y. Aygörmöz and M. Bayati, "Combined effect of using steel fibers and demolition waste aggregates on the performance of fly ash/slag based geopolymer concrete," *European Journal of Environmental and Civil Engineering*, pp. 1-28, 3 2023.
- [2] Ş. O. Demirel C., "Erken Yaşdaki Atık Betonların Geri Dönüşüm Agregası Olarak Beton Üretiminde Kullanılabilirliği ve Sürdürülebilirlik Açısından İncelenmesi.," *Düzce Üniversitesi Bilim ve Teknoloji Dergisi*, no. 3, pp. 226-235, 2015.
- [3] F. Sahin, M. Uysal, O. Canpolat, T. Cosgun and H. Dehghanpour, "The effect of polyvinyl fibers on metakaolin-based geopolymer mortars with different aggregate filling," *Construction and Building Materials*, vol. 300, 9 2021.
- [4] X. Zheng, J. Zhang, X. Ding, H. Chu and J. Zhang, "Frost resistance of internal curing concrete with calcined natural zeolite particles," *Construction and Building Materials*, vol. 288, 6 2021.
- [5] C. Florez, O. Restrepo-Baena and J. I. Tobon, "Effects of calcination and milling pre-treatments on natural zeolites as a supplementary cementitious material," *Construction and Building Materials*, vol. 310, 12 2021.
- [6] A. Nikolov, H. Nugteren and I. Rostovsky, "Optimization of geopolymers based on natural zeolite clinoptilolite by calcination and use of aluminate activators," *Construction and Building Materials*, vol. 243, 5 2020.
- [7] S. Özen and B. Alam, "Compressive strength and microstructural characteristics of natural zeolite-based geopolymer," *Periodica Polytechnica Civil Engineering*, vol. 62, no. 1, pp. 64-71, 2018.
- [8] Y. Aygörmöz, "Performance of ambient and freezing-thawing cured metazeolite and slag based geopolymer composites against elevated temperatures," *Revista de la Construcción*, vol. 20, no. 1, pp. 145-162, 2021.
- [9] R. R. Bellum, "Influence of steel and PP fibers on mechanical and microstructural properties of fly ash-GGBFS based geopolymer composites," *Ceramics International*, vol. 48, no. 5, pp. 6808-6818, 3 2022.

- [10] O. Abdulkareem and J. Matthews, "Improving the Mechanical Strengths of Hybrid Waste Geopolymer Binders by Short Fiber Reinforcement," *Arabian Journal for Science and Engineering*, vol. 46, no. 5, pp. 4781-4789, 2021.
- [11] Y. Alrefaei and J.-G. Dai, "Tensile behavior and microstructure of hybrid fiber ambient cured one-part engineered geopolymer composites," *Construction and Building Materials*, vol. 184, pp. 419-431, 2018.
- [12] F. Amalia, N. Akifah, Nurfadilla and Subaer, "Development of coconut trunk fiber geopolymer hybrid composite for structural engineering materials," *IOP Conference Series: Materials Science and Engineering*, vol. 180, no. 1, 2017.
- [13] K. Arunkumar, M. Muthukannan, A. Sureshkumar, A. Chithambarganesh and R. Rangaswamy Kanniga Devi, "Mechanical and durability characterization of hybrid fibre reinforced green geopolymer concrete," *Research on Engineering Structures and Materials*, vol. 8, no. 1, pp. 19-43, 2022.
- [14] P. Nuaklong, A. Wongsas, K. Boonserm, C. Ngohpok, P. Jongvivatsakul, V. Sata, P. Sukontasukkul and P. Chindaprasirt, "Enhancement of mechanical properties of fly ash geopolymer containing fine recycled concrete aggregate with micro carbon fiber," *Journal of Building Engineering*, vol. 41, 9 2021.
- [15] W. Punurai, W. Kroehong, A. Saptamongkol and P. Chindaprasirt, "Mechanical properties, microstructure and drying shrinkage of hybrid fly ash-basalt fiber geopolymer paste," *Construction and Building Materials*, vol. 186, pp. 62-70, 2018.
- [16] W. H. Sachet and W. D. Salman, "Compressive Strength Development of Slag-Based Geopolymer Paste Reinforced with Fibers Cured at Ambient Condition," *IOP Conference Series: Materials Science and Engineering*, vol. 928, no. 2, 11 2020.
- [17] K. Zada Farhan, M. Azmi Megat Johari and R. Demirboğa, "Evaluation of properties of steel fiber reinforced GGBFS-based geopolymer composites in aggressive environments," *Construction and Building Materials*, vol. 345, p. 128339, 8 2022.
- [18] M. Frydrych, S. Hýsek, L. Fridrichová, S. Van, M. Herclík, M. Pechociaková, H. Chi and P. Louda, "Impact of flax and basalt fibre reinforcement on selected properties of geopolymer composites," *Sustainability (Switzerland)*, vol. 12, no. 1, 2020.
- [19] X. Gao, Q. Yu, R. Yu and H. Brouwers, "Evaluation of hybrid steel fiber reinforcement in high performance geopolymer composites," *Materials and Structures/Materiaux et Constructions*, vol. 50, no. 2, 2017.
- [20] S. Guler and Z. F. Akbulut, "Effect of high-temperature on the behavior of single and hybrid glass and basalt fiber added geopolymer cement mortars," *Journal of Building Engineering*, vol. 57, p. 104809, 10 2022.
- [21] C. Le, P. Louda, K. Buczkowska and I. Dufkova, "Investigation on flexural behavior of geopolymer-based carbon textile/basalt fiber hybrid composite," *Polymers*, vol. 13, no. 5, pp. 1-18, 2021.
- [22] V. Sathish Kumar, N. Ganesan and P. Indira, "Effect of hybrid fibres on the durability characteristics of ternary blend geopolymer concrete," *Journal of Composites Science*, vol. 5, no. 10, 2021.
- [23] A. Baziak, K. Pławecka, I. Hager, A. Castel and K. Korniejenko, "Development and characterization of lightweight geopolymer composite reinforced with hybrid carbon and steel," *Materials*, vol. 14, no. 19, 2021.
- [24] A. Chithambar Ganesh and M. Muthukannan, "Experimental Study on the Behaviour of Hybrid Fiber Reinforced Geopolymer Concrete under Ambient Curing Condition," *IOP Conference Series: Materials Science and Engineering*, vol. 561, no. 1, 11 2019.
- [25] D. Jia, P. He, M. Wang and S. Yan, Short SiC Fiber and Hybrid SiC/Carbon Fiber Reinforced Geopolymer Matrix Composites, vol. 311, 2020, pp. 243-270. [10.1007/978-981-15-9536-3_7](https://doi.org/10.1007/978-981-15-9536-3_7).
- [26] J. Junior, A. Saha, P. Sarker and A. Pramanik, "Workability and flexural properties of fibre-reinforced geopolymer using different mono and hybrid fibres," *Materials*, vol. 14, no. 16, 2021.
- [27] M. Maras, "Tensile and flexural strength cracking behavior of geopolymer composite reinforced with hybrid fibers," *Arabian Journal of Geosciences*, vol. 14, no. 22, 2021.
- [28] P. Sukontasukkul, P. Pongsopha, P. Chindaprasirt and S. Songpiriyakij, "Flexural performance and toughness of hybrid steel and polypropylene fibre reinforced geopolymer," *Construction and Building Materials*, vol. 161, pp. 37-44, 2 2018.
- [29] N. P. Asrani, G. Murali, K. Parthiban, K. Surya, A. Prakash, K. Rathika and U. Chandru, "A feasibility of enhancing the impact resistance of hybrid fibrous geopolymer composites: Experiments and modelling," *Construction and Building Materials*, vol. 203, pp. 56-68, 4 2019.
- [30] J. I. Choi, H. H. Nguyễn, S. E. Park, R. Ranade and B. Y. Lee, "Effects of fiber hybridization on mechanical properties and autogenous healing of alkali-activated slag-based composites," *Construction and Building Materials*, vol. 310, 12 2021.
- [31] F. U. A. Shaikh, "Tensile and flexural behaviour of recycled polyethylene terephthalate (PET) fibre reinforced geopolymer composites," *Construction and Building Materials*, vol. 245, 6 2020.
- [32] A. B. Malkawi, M. F. Nuruddin, A. Fauzi, H. Almattarneh and B. S. Mohammed, "Effects of Alkaline Solution on Properties of the HCFA

- Geopolymer Mortars," *Procedia Engineering*, vol. 148, pp. 710-717, 2016.
- [33] R. K. Chaithanya, C. V. Reddy, L. S. Reddy and K. T. Kumar, "Effect Of Molarity On Strength Characteristics Of Geopolymer Mortar Based On Fly ash and GGBS". *Solid State Technology*. (2020), 63(2s).
- [34] S. Singh, M. U. Aswath and R. V. Ranganath, "Performance assessment of bricks and prisms: Red mud based geopolymer composite," *Journal of Building Engineering*, vol. 32, 11 2020.
- [35] M. Mudgal, A. Singh, R. K. Chouhan, A. Acharya and A. K. Srivastava, "Fly ash red mud geopolymer with improved mechanical strength," *Cleaner Engineering and Technology*, vol. 4, 10 2021.
- [36] Y. Aygörmez, "Assessment of performance of metabentonite and metazeolite-based geopolymers with fly ash sand replacement," *Construction and Building Materials*, vol. 302, 10 2021.
- [37] Y. Aygörmez, "Evaluation of the red mud and quartz sand on reinforced metazeolite-based geopolymer composites," *Journal of Building Engineering*, vol. 43, 11 2021.
- [38] U. Zakira, K. Zheng, N. Xie and B. Birgisson, "Development of high-strength geopolymers from red mud and blast furnace slag," *Jour. of Clean. Prod.*, vol. 383, 1 2023.
- [39] M. Uysal, Ö. Faruk Kuranlı, Y. Aygörmez, O. Canpolat and T. Çoşgun, "The effect of various fibers on the red mud additive sustainable geopolymer composites," *Cons. and Buil. Mat*, vol. 363, 1 2023.
- [40] T. Alomayri and I. M. Low, "Synthesis and characterization of mechanical properties in cotton fiber-reinforced geopolymer composites," *Journal of Asian Ceramic Societies*, vol. 1, no. 1, pp. 30-34, 2013.
- [41] T. Alomayri, F. U. Shaikh and I. M. Low, "Characterisation of cotton fibre-reinforced geopolymer composites," *Composites Part B: Engineering*, vol. 50, pp. 1-6, 7 2013.
- [42] H. Baykara, M. H. Cornejo, A. Espinoza, E. García and N. Ulloa, "Preparation, characterization, and evaluation of compressive strength of PFRGM," *Heliyon*, vol. 6, no. 4, 4 2020.